

## Probing intrinsic polarization properties in bismuth-layered ferroelectric films

Takayuki Watanabe<sup>a)</sup> and Hiroshi Funakubo

*Department of Innovative and Engineered Materials, Tokyo Institute of Technology, Yokohama 226-8502, Japan*

Minoru Osada

*Nanoscale Materials Center, National Institute for Materials Science (NIMS), Tsukuba 305-0044, Japan*

Hiroshi Uchida and Isao Okada

*Department of Chemistry, Sophia University, Tokyo 102-8554, Japan*

Brian J. Rodriguez<sup>b)</sup> and Alexei Gruverman

*Department of Materials Science and Engineering, North Carolina State University, Raleigh, North Carolina 27695*

(Received 9 December 2006; accepted 10 February 2007; published online 16 March 2007)

The authors report on an approach to establish intrinsic polarization properties in bismuth-layered ferroelectric films by piezoelectric coefficient and soft-mode spectroscopy, as well as by a direct polarization–electric field hysteresis. In epitaxially grown  $(\text{Bi}_{4-x}\text{Nd}_x)\text{Ti}_3\text{O}_{12}$  ( $0 \leq x \leq 0.73$ ) films, they show that these complementary characterizations can phenomenologically and thermodynamically represent the intrinsic polarization states in  $(\text{Bi}_{4-x}\text{Nd}_x)\text{Ti}_3\text{O}_{12}$  films, and the intrinsic  $P_s$  of  $67 \mu\text{C}/\text{cm}^2$  is estimated for pure  $\text{Bi}_4\text{Ti}_3\text{O}_{12}$ , superior to  $50 \mu\text{C}/\text{cm}^2$  in bulk single crystal. Their results provide a pathway to draw full potential in ferroelectric thin films. © 2007 American Institute of Physics. [DOI: 10.1063/1.2713858]

Polarization reversals in ferroelectrics have been the topic of intensive study due to their potential applications in memory storage and integrated microelectronics.<sup>1</sup>  $\text{Bi}_4\text{Ti}_3\text{O}_{12}$  (BIT) has a pronounced spontaneous polarization ( $P_s$ ) along the  $a$  axis, which is known to be the largest so far in the series of layered ferroelectrics. Cummins and Cross reported the  $P_s$  of  $50 \pm 10 \mu\text{C}/\text{cm}^2$  along the  $a$  axis for a bulk single crystal BIT,<sup>2</sup> while they noted that this would be the minimum value because of the difficulty in confirming the full switching of the intrinsic  $P_s$ . On the other hand, substitution techniques using lanthanoid and higher-valent cation is widely performed to compensate for defects or the complexes.<sup>3–5</sup> The substitution techniques improve the apparent ferroelectricity, but it has not been clarified yet how the substitution affects the  $P_s$ . We perform combined electrical, electromechanical, and optical approaches for 400-nm-thick (110) $(\text{Bi}_{4-x}\text{Nd}_x)\text{Ti}_3\text{O}_{12}$  (BNT) ( $0 \leq x \leq 0.73$ ) epitaxial thin films<sup>6</sup> to establish the intrinsic  $P_s$  of the films.

The  $P_s$  [or saturation polarization ( $P_{\text{sat}}$ ) if the electric field was not applied along the spontaneous polar axis] is defined as a  $y$  intercept of a tangent drawn to a polarization–electric field ( $P$ – $E$ ) hysteresis loop. On the other hand, piezoelectric coefficient and soft-mode frequency are correlated with the polarization.

The effective piezoelectric coefficient  $d$  is designated as

$$d = 2Q\varepsilon_0\varepsilon P, \quad (1)$$

consisting of  $Q$  the electrostriction coefficient,  $\varepsilon_0\varepsilon$  the dielectric constant, and  $P$  the polarization.<sup>7</sup> Assuming a con-

stant electrostriction coefficient, we can estimate the relative amplitude of the remanent polarization ( $P_r$ ) from the effective piezoelectric coefficient, e.g., effective  $d_{33}$ , at zero bias field. An inverse piezoelectric response was recorded using piezoresponse force microscopy (PFM), where the tip is in contact with the ferroelectric layer without top electrodes. In this study, we would treat a direct electric signal from the PFM in unit of millivolts instead of an effective  $d_{33}$  value that may be converted from the signal with a force curve measurement. The standard deviation in the PFM measured  $d_{33}$  value of a single grain does not exceed 10%.

Mean field theory describes  $P_s$  ( $T <$  Curie temperature  $T_C$ ) as a function of the soft-mode frequency,<sup>8</sup> which is expressed by

$$M\omega(q)^2 = 2\gamma\langle Q \rangle^2 + (\nu_0 - \nu_q), \quad (2)$$

consisting of  $M$  the mass of the ions related to soft mode,  $\omega(q)$  the soft-mode frequency,  $\gamma$  the anharmonic ratio,  $\langle Q \rangle$  the order parameter,  $P_s$ , and  $(\nu_0 - \nu_q)$  is a correction term for the third-order anharmonics and a long-range interaction. In the case of displacive-type ferroelectrics, a short-range interaction is mainly responsible for the soft mode, so that the last correction term can be ignored. Therefore,  $P_s^2$  is a function of square of the soft-mode frequency,<sup>9</sup> which can be identified by Raman scattering.<sup>6</sup> These approaches will provide complementary information to a  $P$ – $E$  hysteresis measurement for probing  $P_s$ .

Figure 1 shows  $P$ – $E$  hysteresis loops of (110)BNT films measured via circular Pt top electrodes of 100  $\mu\text{m}$  in diameter. No  $P$ – $E$  hysteresis was observed for pure BIT film because of the low resistivity. The estimated  $P_{\text{sat}}$  reached the maximum at around  $x=0.26$ – $0.35$ , then significantly dropped with the incorporation of Nd into the  $(\text{Bi}_2\text{O}_2)^{2+}$

<sup>a)</sup>Also at Institute of Solid State Physics and CNI (Center of Nanoelectronic Systems for Information Technology), Research Center Jülich, 52425 Jülich, Germany; electronic mail: t.watanabe@fz-juelich.de

<sup>b)</sup>Present address: Oak Ridge National Laboratory, Oak Ridge, Tennessee 37831.

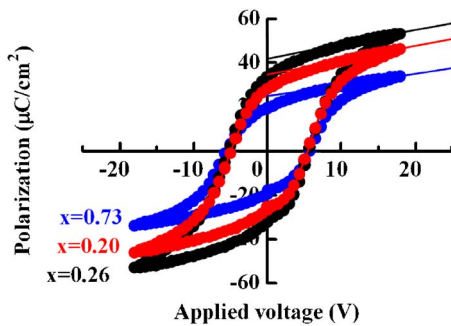


FIG. 1. (Color online) Polarization-electric field hysteresis loops of as-deposited epitaxial (110)(Bi<sub>4-x</sub>Nd<sub>x</sub>)Ti<sub>3</sub>O<sub>12</sub> ( $x=0.2, 0.26,$  and  $0.73$ ) films measured with a 20 Hz triangular wave.

layer at  $x=0.73$ .<sup>6</sup> The estimated  $P_{\text{sat}}$  for (110)BNT films is converted to  $P_s$  along the  $a$  axis by multiplying by root 2 and summarized into Fig. 4.

Figure 2 depicts two-dimensional piezoresponse and the phase in  $10 \mu\text{m}^2$  for the BIT film and in  $5 \mu\text{m}^2$  for the BNT films. In the surface topographic images (not shown here), the films consisted of distinctive needlelike grains forming in-plane  $c$ -axis-oriented films.<sup>10</sup> Prior to piezoresponse measurements, the films were poled by a dc field with amplitude

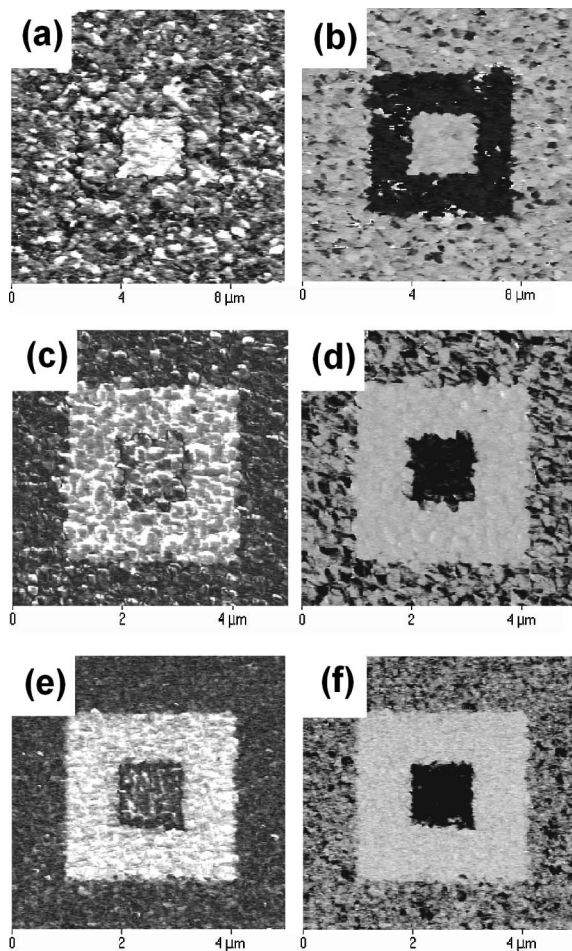


FIG. 2. Piezoresponse (left string) and the phase (right string) of epitaxial (110)(Bi<sub>4-x</sub>Nd<sub>x</sub>)Ti<sub>3</sub>O<sub>12</sub> films ( $x=0, 0.2,$  and  $0.42$ ). [(a), (b)]  $x=0$ , [(c), (d)]  $x=0.2$ , and [(e), (f)]  $x=0.42$ . The quasistatic inverse piezoelectric response against a dc bias superimposed on a weak ac field (amplitude: 1.5 V; frequency 10 kHz) was recorded by piezoresponse force microscopy. The bright and dark region in the phase images correspond to downward and upward polarization states, respectively.

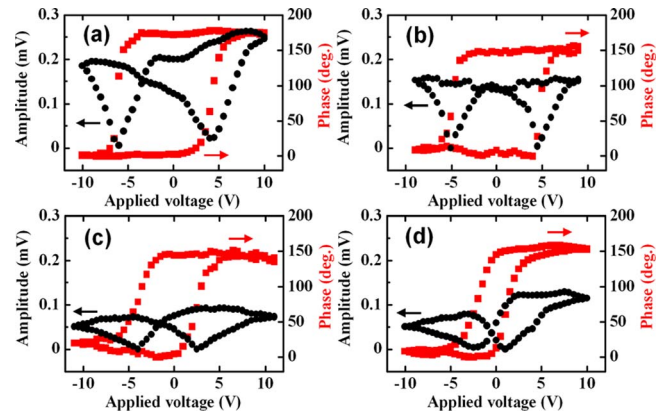


FIG. 3. (Color online) Static piezoresponse and the phase of the epitaxial (110)(Bi<sub>4-x</sub>Nd<sub>x</sub>)Ti<sub>3</sub>O<sub>12</sub> films. (a)  $x=0$ , (b)  $x=0.2$ , (c)  $x=0.42$ , and (d)  $x=0.73$ . The piezoresponse force microscope measurement was performed with a dc bias superimposed on a weak ac field (amplitude: 1.5 V; frequency 10 kHz) directly on the film surface without the top electrode.

of  $\pm 10$  V in a concentric double square shape, and the outer part was left without the poling treatment. Looking at the piezoresponse of the BIT film in Fig. 2(a), the center part poled by the positive dc bias showed a homogeneous piezoresponse. In contrast, an inhomogeneous piezoresponse, which is identical to that at the outside nonpoled region, was observed for the area poled with the negative dc bias. Interestingly, the phase image [Fig. 2(b)] showed that the net polarization was homogeneously aligned along the applied dc bias irrespective of the poling direction. The outside nonpoled area is preferably polarized downward without the poling operation.

These PFM measurements indicate that the BIT film had an internal bias field towards the bottom electrode, which arises from Schottky barrier between the ferroelectric layer with semiconductor properties and the bottom electrode.<sup>11,12</sup> This built-in field pointing to the bottom electrode assists in switching the polarization towards the bottom electrode by a positive electric field but in return hampers an upward full switching. The inhomogeneous piezoresponse in the negatively poled region reveals that the amplitude of the internal bias field had a large distribution.<sup>11</sup> The present downward internal bias field indicates that the BIT had a  $n$ -type character at the interface with the bottom electrode probably because of oxygen vacancies. With the Nd substitution, the poled region showed uniform piezoresponse and the nonpoled region presented nearly equal upward and downward polarization states as can be seen in Figs. 2(c)–2(f). The internal bias field appears to be homogenized or reduced by the Nd substitution. However, a slight internal bias aligned to the bottom electrode is still expected, because the positively poled region always exhibited larger piezoresponse comparing to the negatively poled region.

Figure 3 shows the amplitude and the phase of a quasistatic piezoresponse as a function of the dc bias. Due to the downward internal bias field, the piezoelectric hysteresis loops have negative field offset. The BNT films with  $x \geq 0.42$  showed significantly smaller average coercive voltage ( $V_c$ ) in the piezoresponse hysteresis loops than those in the  $P$ - $E$  hysteresis loops. This discrepancy in the  $V_c$  is often observed;<sup>12,13</sup> however, the reason for the present case is not clear. Probably, the switching mechanism is different for the microscopic PFM and macroscopic  $P$ - $E$  measurements. Ac-

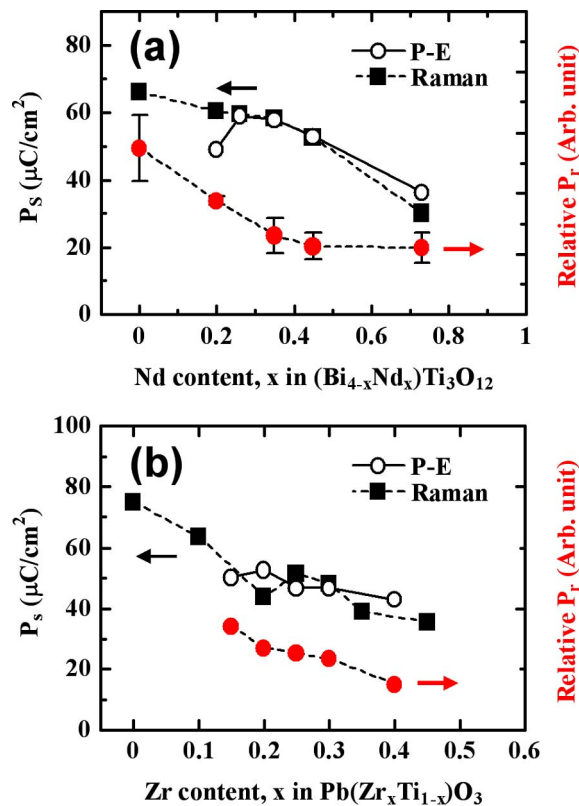


FIG. 4. (Color online) Spontaneous polarization (a) along the  $a$  axis of  $(110)(\text{Bi}_{4-x}\text{Nd}_x)\text{Ti}_3\text{O}_{12}$  films and (b) along the  $c$ -axis of  $(111)\text{Pb}(\text{Zr}_x\text{Ti}_{1-x})\text{O}_3$  films (Ref. 16) estimated from the polarization–electric field hysteresis, piezoresponse force microscopy, and Raman measurements.

According to Eq. (1), the piezoresponse amplitude at zero field is associated to  $P_r$ . With an assumption of an independent electrostrictive coefficient of the Nd content for the BNT films, we can see the relative  $P_r$  of the BNT films by dividing the piezoresponse amplitude by the relative dielectric constant.

Figure 4(a) summarizes  $P_s$  estimated by the  $P$ - $E$  hysteresis loops and relative  $P_r$  given by the piezoresponse measurements. In the figure, relative  $P_s$  values calculated from the square of soft-mode frequency were also displayed. The three polarizations exhibited a nearly identical behavior against the amount of Nd substitution. For the optically obtained relative  $P_s$ , we gave a factor as it agrees with the absolute  $P_s$  values given by the  $P$ - $E$  hysteresis loops, so that the optical  $P_s$  for BIT reached  $\sim 67 \mu\text{C}/\text{cm}^2$ .

As decreasing Nd content, the  $P_s$  estimated from the  $P$ - $E$  hysteresis loops increased and then decreased at  $x=0.2$ . On the other hand, both of the relative  $P_r$  provided by the PFM measurements and the  $P_s$  estimated by Raman scattering strongly suggest that the intrinsic  $P_s$  will be maximum at  $x=0$ . The capacitors with Pt top electrode pads used for the  $P$ - $E$  measurements would have an internal field at the top interface as well as the bottom interface.<sup>14</sup> Because an obvious transverse offset was not observed for the  $P$ - $E$  hysteresis loops for the BNT films, the direction of the top internal field is considered to be upward. The double depletion layer can potentially pin the sandwiched polarization to interfere the reorientation of polarization as well as the defect complexes.

This phenomenon will be more serious as the film thickness decreases.<sup>15</sup>

To assess the generality of the present approach, the same technique was applied to other ferroelectrics with different crystal structures, perovskite  $\text{Pb}(\text{Zr}_x\text{Ti}_{1-x})\text{O}_3$  (PZT). Figure 4(b) summarizes the trend of  $P_s$  estimated from (111)-textured PZT films<sup>16</sup> and PZT powder<sup>17</sup> as a function of the Zr content. The absolute  $P_s$  along the  $c$  axis was obtained by dividing the  $P_{\text{sat}}$  of the (111)-textured PZT films by  $\cos 54.7^\circ$ . The relative  $P_r$  was obtained by dividing the piezoresponse amplitude by the relative dielectric constant of the PZT films. The relative  $P_s$  calculated from the soft mode was adjusted as it gets  $75 \mu\text{C}/\text{cm}^2$  at  $x=0$ , which was reported for single crystal  $\text{PbTiO}_3$ .<sup>18</sup> The polarization values estimated by different methods again appeared to be in sync with each other depending on the Zr content.

In summary, we have examined intrinsic polarization properties of  $(\text{Bi}_{4-x}\text{Nd}_x)\text{Ti}_3\text{O}_{12}$  by the  $P$ - $E$  hysteresis, PFM, and Raman measurements and found that these techniques based on different theories can complementarily approach the intrinsic polarization of ferroelectrics. Concerning the bismuth-layered ferroelectrics, it was shown that the lanthanoid substitutions release the fixed polarization sacrificing the large  $P_s$  of  $67 \mu\text{C}/\text{cm}^2$  of BIT. Another substitution element or electrode structure, which can effectively compensate for the defects and internal bias field, is highly demanded for these lead-free and high-working temperature ferroelectric devices.

One of the authors (T.W.) is grateful for receiving a research fellowship from the Japan Society for the Promotion of Science for Young Scientists. A.G. acknowledges support by the National Science Foundation (Grant No. DMR-0235632).

- <sup>1</sup>J. F. Scott and C. A. Araujo, *Science* **246**, 1400 (1989).
- <sup>2</sup>S. E. Cummins and L. E. Cross, *J. Appl. Phys.* **39**, 2268 (1968).
- <sup>3</sup>Y. Noguchi, I. Miwa, Y. Goshima, and M. Miyayama, *Jpn. J. Appl. Phys., Part 2* **39**, L1259 (2000).
- <sup>4</sup>B. H. Park, B. S. Kang, S. D. Bu, T. W. Noh, L. Lee, and W. Joe, *Nature (London)* **401**, 682 (1999).
- <sup>5</sup>T. Noguchi and M. Miyayama, *Appl. Phys. Lett.* **78**, 1903 (2001).
- <sup>6</sup>T. Watanabe, H. Funakubo, M. Osada, H. Uchida, and I. Okada, *J. Appl. Phys.* **98**, 024110 (2005).
- <sup>7</sup>D. Damjanovic, *Rep. Prog. Phys.* **61**, 1267 (1998).
- <sup>8</sup>R. Blinc, and B. Žeks, *Soft Modes in Ferroelectrics and Antiferroelectrics* (North-Holland, Amsterdam, 1974).
- <sup>9</sup>S. Kojima, R. Imaizumi, S. Hamazaki, and M. Takashige, *Jpn. J. Appl. Phys., Part 1* **33**, 5559 (1994).
- <sup>10</sup>H. N. Lee, D. Hesse, N. Zakharov, and U. Gösele, *Science* **296**, 2006 (2002).
- <sup>11</sup>A. Gruverman, A. Kholkin, A. Kingon, and H. Tokumoto, *Appl. Phys. Lett.* **78**, 2751 (2001).
- <sup>12</sup>S. Hiboux, P. Muralt, and T. Maeder, *J. Mater. Res.* **14**, 4307 (1999).
- <sup>13</sup>V. V. Shvartsman, N. A. Pertsev, J. M. Herrero, C. Zaldo, and A. L. Kholkin, *J. Appl. Phys.* **97**, 104105 (2005).
- <sup>14</sup>B. H. Park, S. J. Hyun, C. R. Moon, B.-D. Choe, J. Lee, C. Y. Kim, W. Jo, and T. W. Noh, *J. Appl. Phys.* **84**, 4428 (1998).
- <sup>15</sup>T. Watanabe, A. Saiki, K. Saito, and H. Funakubo, *J. Appl. Phys.* **89**, 3934 (2001).
- <sup>16</sup>D. J. Kim, J. P. Maria, A. I. Kingon, and S. K. Streiffer, *J. Appl. Phys.* **93**, 5568 (2003).
- <sup>17</sup>D. Bäuerle, Y. Yacoby, and W. Richter, *Solid State Commun.* **14**, 1137 (1974).
- <sup>18</sup>V. G. Gavrilachenko, R. I. Spinko, M. A. Martynenko, and E. G. Fesenko, *Sov. Phys. Solid State* **12**, 1203 (1970).